

Dynamic modeling of cavitation bubble clusters: Effects of evaporation, condensation, and bubble—bubble interaction

Long Xu(许龙), Xin-Rui Yao(姚昕锐), and Yang Shen(沈阳)

Citation: Chin. Phys. B, 2024, 33 (**4**): 044702. DOI: 10.1088/1674-1056/ad181f
Journal homepage: http://cpb.iphy.ac.cn; http://iopscience.iop.org/cpb

What follows is a list of articles you may be interested in

Effect of non-condensable gas on a collapsing cavitation bubble near solid wall investigated by multicomponent thermal MRT-LBM

Yu Yang(杨雨), Ming-Lei Shan(单鸣雷), Qing-Bang Han(韩庆邦), and Xue-Fen Kan(阚雪芬)
Chin. Phys. B, 2021, 30 (**2**): 024701. DOI: 10.1088/1674-1056/abbbf8

Multi-bubble motion behavior of uniform magnetic field based on phase field model

Chang-Sheng Zhu(朱昶胜), Zhen Hu(胡震), Kai-Ming Wang(王凯明)
Chin. Phys. B, 2020, 29 (**3**): 034702. DOI: 10.1088/1674-1056/ab6839

Multi-bubble motion behavior of electric field based on phase field model

Chang-Sheng Zhu(朱昶胜), Dan Han(韩丹), Li Feng(冯力), Sheng Xu(徐升)
Chin. Phys. B, 2019, 28 (**3**): 034701. DOI: 10.1088/1674-1056/28/3/034701

Phase field simulation of single bubble behavior under an electric field

Chang-Sheng Zhu(朱昶胜), Dan Han(韩丹), Sheng Xu(徐升)
Chin. Phys. B, 2018, 27 (**9**): 094704. DOI: 10.1088/1674-1056/27/9/094704

Pseudopotential multi-relaxation-time lattice Boltzmann model for cavitation bubble collapse with high density ratio

Ming-Lei Shan(单鸣雷), Chang-Ping Zhu(朱昌平), Cheng Yao(姚澄), Cheng Yin(殷澄), Xiao-Yan Jiang(蒋小燕)
Chin. Phys. B, 2016, 25 (**10**): 104701. DOI: 10.1088/1674-1056/25/10/104701

Dynamic modeling of cavitation bubble clusters: Effects of evaporation, condensation, and bubble–bubble interaction

Long Xu(许龙)[†], Xin-Rui Yao(姚昕锐), and Yang Shen(沈阳)

College of Science, China Jiliang University, Hangzhou 310018, *China*

(Received 24 October 2023; revised manuscript received 14 December 2023; accepted manuscript online 22 December 2023)

We present a dynamic model of cavitation bubbles in a cluster, in which the effects of evaporation, condensation, and bubble–bubble interactions are taken into consideration. Under different ultrasound conditions, we examine how the dynamics of cavitation bubbles are affected by several factors, such as the locations of the bubbles, the ambient radius, and the number of bubbles. Herein the variations of bubble radius, energy, temperature, pressure, and the quantity of vapor molecules are analyzed. Our findings reveal that bubble–bubble interactions can restrict the expansion of bubbles, reduce the exchange of energy among vapor molecules, and diminish the maximum internal temperature and pressure when bursting. The ambient radius of bubbles can influence the intensities of their oscillations, with clusters comprised of smaller bubbles creating optimal conditions for generating high-temperature and high-pressure regions. Moreover, an increase in the number of bubbles can further inhibit cavitation activities. The frequency, pressure and waveform of the driving wave can also exert a significant influence on cavitation activities, with rectangular waves enhancing and triangular waves weakening the cavitation of bubbles in the cluster. These results provide a theoretical basis for understanding the dynamics of cavitation bubbles in a bubble cluster, and the factors that affect their behaviors.

Keywords: bubble dynamics, bubble–bubble interaction, mass exchange, ultrasound waveform

PACS: 47.55.dd, 43.35.+d **DOI:** 10.1088/1674-1056/ad181f

1. Introduction

Cavitation is a phenomenon that occurs when cavities form and collapse in a liquid due to a drop in pressure.[1] The collapse of these bubbles generates high temperatures and pressures, as well as various physical effects such as shock waves, microjets, and acoustic luminescence.[2–5] Due to these extreme conditions, ultrasonic cavitation has been widely used in environmental engineering, biomedical engineering, material science, and food processing.[6–9] Understanding the dynamic behaviors of bubbles in different environments is a topic of ongoing research, as the cavitation mechanism is closely related to bubble dynamics.

The dynamics of a single bubble has been studied extensively since Rayleigh formulated the basic dynamical equation for a spherical bubble in an unbounded flow field.[10] However, the original equation ignored critical factors such as surface tension, liquid viscosity, and external sound pressure. Subsequent researchers have refined the Rayleigh equation by incorporating additional factors, including surface tension at the gas–liquid interface and liquid viscosity.[11–13] Further advances include the incorporation of the compressibility of the liquid and the radiation damping of bubble oscillation into the theoretical model.[14] Yasui[15] extended the model to thermal effects and evaporation/condensation of water vapor, resulting in a more completely theoretical framework. Lu *et al.*[16] proposed a new numerical method, the conduction-radiation method, in which the heat conduction effect and thermal radiation effect are taken into consideration for simulating cavitation bubbles, and the results are highly consistent with experimental observations. Gao *et al.*[17] established a mass transfer model to investigate the relationship between the equilibrium radius and the driving ultrasound, and they also measured the bubble radius evolution in sulfuric acid driven by ultrasound. The experimental result is consistent with the simulation result. To accurately calculate the pressures and temperatures at the bubble wall and in the liquid adjacent to the wall just before and after the collapse, Cogné *et al.*[18] presented two methods of modeling the heat transfer between liquid and a single bubble, and the precise pressure and temperature distributions in the cavitation area were obtained. In addition to the above studies, the dynamics of a cavitation bubble was investigated by introducing different types of driving ultrasounds. Liao *et al.*[19] calculated the effects of frequency difference, phase difference, and power allocation ratio on the acoustic cavitation under dual-frequency ultrasound, and the results showed that the cavitation activities are obviously enhanced by the dual-frequency ultrasound with a small frequency difference. Suo *et al.*[20] conducted a numerical investigation on the inertial cavitation threshold of bubbles caused by multi-frequency ultrasound, and thus providing a possible approach to optimizing ultrasound excitations for inducing cavitation. Wang *et al.*[21] analyzed the effect of the interaction between bubbles on the scattered acoustic pressure under dual-frequency ultrasound by solving the dynamic equation of bubble oscillation in viscoelastic tissues, and they found that as the frequency

[†]Corresponding author. E-mail: xulong@cjlu.edu.cn

© 2024 Chinese Physical Society and IOP Publishing Ltd

of driving acoustic wave approaches the resonant frequency of the bubble, the interaction between two bubbles with the same size will suppress the oscillations of the bubbles.

However, in practice, cavitation typically occurs in the form of clusters, and thus the dynamics of multiple cavitation bubbles have been studied. Early studies by Bjerknes[22] revealed that bubbles in an acoustic field exhibit mutual interaction. This discovery prompted many researchers to explore the behavior of interacting bubbles both experimentally and theoretically.[23–27] Shen *et al.*[27] investigated the effect of the interaction between bubbles on the radial pulsation of bubbles, and the obtained results showed that the radiated pressure waves can not only suppress expansion ratio of bubble, but also enlarge that of bubble. Qin *et al.*[28] compared the amplitude and nonlinearity of the bubble oscillation without and with the inter-bubble interaction, and found that the interaction between bubbles can enhance or suppress the amplitude and nonlinearity of the bubbles' oscillation. Zou *et al.*[29] analyzed the effects of the size polydispersity and two-dimensional (2D) structure of bubbles on bubble pulsation characteristics in a three-bubble system. Despite the fact that some of these studies established multi-bubble models, they did not consider mass exchange between the inside and outside of the cavitation bubble nor the interaction between neighboring bubbles. In order to achieve a more comprehensive understanding of ultrasonic cavitation dynamics, we present a model that takes into consideration the evaporation and condensation of water vapor, as well as the interaction between neighboring bubbles in a spherical cluster. Our model allows for the analysis of a bubble at any position within the cluster, thus improving understanding of ultrasonic cavitation behavior. The rest of this paper is organized as follows. In Section 2, the justification of our model's assumptions and the description of the derivation process, including approaches to calculating energy, temperature, and pressure inside the bubble, are provided. A coupling variable is introduced into the model to simulate the interactions between bubbles in the cluster. In Section 3, the physical parameters used in our calculations are presented. Nonlinear bubble oscillations are investigated, and the influences of bubble positions, the number of bubbles, and the ambient radius on their dynamic behavior are explored. Various ultrasonic waveforms are introduced as excitation to investigate the response of bubbles to different acoustic fields, including changes in radius, internal energy, internal temperature, internal pressure, and the number of water vapor molecules. Finally, in Section 4, some conclusions are drawn from the present study.

2. Model

In order to establish the vibration model of a cavitation bubble in a spherical cluster, in which the exchange between internal mass and external mass is considered, seven assumptions are made as follows. The first assumption is that the influence of the boundary movement on the pressure distribution in the cluster is not considered; the second one is that bubbles are always spherically symmetrical and only pulsated in the radial direction; the third one is that the radius of the spherical cluster is relatively small compared with the wavelength of the external driving acoustic; the fourth one is that the ambient pressure and the driving acoustic pressure inside the cluster are homogeneous; the fifth one is that the bubbles are distributed uniformly in the cluster with the same ambient radius; the sixth one is that the change of the number of air molecules in the cluster is ignored; the seventh one is that the change in ultrasonic velocity in liquid is neglected.

Based on those assumptions, the motion equation for bubble at any position in the bubble cluster can be expressed as follows:[15]

$$\begin{aligned} &R\ddot{R}\left(1-\frac{\dot{R}}{c}+\frac{\dot{m}}{\rho_0 c}+\frac{3}{2}M\right)+\frac{3}{2}\dot{R}^2\left(1-\frac{\dot{R}}{3c}+\frac{2\dot{m}}{3\rho_0 c}+2M\right)\\ &=\frac{1}{\rho_0}\left(1+\frac{\dot{R}}{c}\right)\left[P_{\rm out}-P_{\rm a}\sin(2\pi f t)-P_0\right]\\ &\quad+\frac{\ddot{m}R}{\rho_0}\left(1-\frac{\dot{R}}{c}+\frac{\dot{m}}{\rho_0 c}\right)+\frac{\dot{m}}{\rho_0}\left(\dot{R}+\frac{\dot{m}}{2\rho_0}+\frac{\dot{R}\dot{m}}{2\rho_0 c}\right)\\ &\quad+\frac{R}{\rho_0 c}\frac{{\rm d}P_{\rm out}}{{\rm d}t}, \end{aligned} \tag{1}$$

where $\cdot$ denotes the time derivative, R the radius of the bubble, c the sound speed in the liquid, $\dot{m}$ the net rate of evaporation per unit area and unit time (when $\dot{m}<0$ indicating the occurrence of condensation), ρ_0 the liquid density, P_0 the ambient pressure, $P_{\rm a}$ the amplitude of the ultrasonic wave, f the frequency of the ultrasonic wave, and[30]

$$M=N\frac{R}{r_{\rm cluster}}\left(1-\frac{r_0^2}{3r_{\rm cluster}^2}\right), \tag{2}$$

with N being the total number of bubbles in the bubble cluster, r_0 the distance between the bubble and the center of the bubble cluster, and $r_{\rm cluster}$ the radius of the spherical cluster, $P_{\rm out}(t)$ related to the pressure inside the bubble $P_{\rm in}(t)$ by

$$P_{\rm out}(t)=P_{\rm in}(t)-\frac{2\sigma}{R}-\frac{4\mu}{R}\left(\dot{R}-\frac{\dot{m}}{\rho_0}\right)-\dot{m}^2\left(\frac{1}{\rho_0}-\frac{1}{\rho_{\rm g}}\right). \tag{3}$$

Here, σ is the surface tension, μ the liquid viscosity, and $\rho_{\rm g}$ the gas density inside the bubble and expressed as

$$\rho_{\rm g}=\frac{M_{\rm H_2O}n_{\rm H_2O}+M_{\rm air}n_{\rm air}}{VN_{\rm A}}, \tag{4}$$

where $M_{\rm H_2O}$ and $M_{\rm air}$ are the molar mass of water vapor and air, respectively, $n_{\rm H_2O}$ and $n_{\rm air}$ the number of water vapor and air in the bubble, V is the volume of the bubble, and $N_{\rm A}$ is the Avogadro's number.

In order to calculate $P_{\rm in}(t)$, the var der Waals equation of state is used:

$$P_{\rm in}(t)=\frac{R_{\rm g}T}{(v-b)}-\frac{a}{v^2}, \tag{5}$$

where a and b are the van der Waals constants, which change with the number of water vapor molecules in the bubble, R_g is the gas constant, T is the temperature inside the bubble, and v is the molar volume. The van der Waals constants are determined by

$$a = a_{\text{air}}\left(\frac{n_{\text{air}}}{n_t}\right)^2 + 2a_{\text{air-H}_2\text{O}}\left(\frac{n_{\text{air}}}{n_t}\right)\left(\frac{n_{\text{H}_2\text{O}}}{n_t}\right) + a_{\text{H}_2\text{O}}\left(\frac{n_{\text{H}_2\text{O}}}{n_t}\right)^2, \tag{6}$$

$$b = b_{\text{air}}\left(\frac{n_{\text{air}}}{n_t}\right)^2 + 2b_{\text{air-H}_2\text{O}}\left(\frac{n_{\text{air}}}{n_t}\right)\left(\frac{n_{\text{H}_2\text{O}}}{n_t}\right) + b_{\text{H}_2\text{O}}\left(\frac{n_{\text{H}_2\text{O}}}{n_t}\right)^2, \tag{7}$$

where a_{air} and b_{air} ($a_{\text{H}_2\text{O}}$ and $b_{\text{H}_2\text{O}}$) are the van der Waals constants of air (water vapor), $a_{\text{air-H}_2\text{O}} = \sqrt{a_{\text{air}}a_{\text{H}_2\text{O}}}$, $\sqrt[3]{b_{\text{air-H}_2\text{O}}} = \frac{1}{2}\left(\sqrt[3]{b_{\text{air}}} + \sqrt[3]{b_{\text{H}_2\text{O}}}\right)$, $n_t = n_{\text{air}} + n_{\text{H}_2\text{O}}$.

The temperature (T) inside the bubble can be calculated from the following equation:[15]

$$T = \frac{N_A^2 EV + \left(n_{\text{H}_2\text{O}} + n_{\text{air}}\right)^2 a}{\left(n_{\text{H}_2\text{O}}C_{\text{V,H}_2\text{O}} + n_{\text{air}}C_{\text{V,air}}\right)N_A V}, \tag{8}$$

where E is the internal energy of the bubble and $C_{\text{V,H}_2\text{O}}$ ($C_{\text{V,air}}$) is the constant molar heat capacity of air (vapor) at temperature T. The change rate of energy (E) per time in the bubble is calculated from[31]

$$\Delta E = -P_{\text{in}}(t)\Delta V(t) + \frac{N_A}{M_{\text{H}_2\text{O}}}4\pi R^2 \dot{m} e \Delta t + 4\pi R^2 \kappa \left.\frac{\partial T}{\partial r}\right|_{r=R}\Delta t, \tag{9}$$

where the first term on the right-hand side of Eq. (9) is the work done by pressure $P_{\text{in}}(t)$ and $\Delta V(t)$ denotes the change in bubble volume with time Δt. The second term is the energy carried by evaporating vapor molecules from the surrounding liquid into the bubble and by condensing vapor molecules from the bubble into the liquid in time Δt. The third term is energy change due to thermal conduction.[32]

It is assumed that temperature in the boundary layer changes linearly with radius. Thus,

$$\left.\frac{\partial T}{\partial r}\right|_{r=R} = \frac{T_B - T}{n\lambda}, \tag{10}$$

where T_B is the gas temperature at the bubble wall, $n\lambda$ the thickness of the boundary layer, n a constant and λ the mean free path of a molecule in the bubble. λ is calculated from

$$\lambda = \frac{V}{\sqrt{2}\sigma' n_t}, \tag{11}$$

where σ' is the cross section of a molecule in the bubble and n_t is the total number of molecules in the bubble.

According to the kinetic theory of gas, the temperature at the bubble wall (T_B) is

$$T_B = T_0 + \Delta T, \tag{12}$$

where T_0 is the liquid temperature and

$$\Delta T = -\frac{1}{2kn'}\sqrt{\frac{\pi m'}{2kT_B}}\frac{2 - a'\alpha_e}{\alpha_e}\kappa \left.\frac{\partial T}{\partial r}\right|_{r=R}. \tag{13}$$

In Eq. (13), k is the Boltzmann constant, n' the number density of gas and vapor molecules in the bubble, m' the mass of one bubble molecule, α_e the thermal accommodation coefficient, a' a constant, and κ the thermal conductivity of the gas.

The thermal conduction coefficient κ is a function of temperature and density of the molecules in the bubble, and the function of temperature is assumed to be linear as follows:[15]

$$\kappa_0 = \alpha T + \beta, \tag{14}$$

where subscript 0 denotes the value at low density. Thermal conductivity of the mixture gas is[15]

$$\kappa_{0,\text{mix}} = \frac{1}{2}\left[\left(\frac{n_{\text{H}_2\text{O}}}{n_t}\kappa_{0,\text{H}_2\text{O}} + \frac{n_{\text{air}}}{n_t}\kappa_{0,\text{air}}\right) + \left(\frac{n_{\text{H}_2\text{O}}}{n_t}\frac{1}{\kappa_{0,\text{H}_2\text{O}}} + \frac{n_{\text{air}}}{n_t}\frac{1}{\kappa_{0,\text{air}}}\right)^{-1}\right], \tag{15}$$

where the subscript H_2O (air) denotes the thermal conductivity of H_2O (air) at low density. The function of heat conduction coefficient κ with respect to density is

$$\kappa = \frac{b}{v}\left(\frac{1}{y} + 1.2 + 0.755y\right)\kappa_{0,\text{mix}}, \tag{16}$$

where

$$y = \left(\frac{b}{v}\right) + 0.625\left(\frac{b}{v}\right)^2 + 0.2869\left(\frac{b}{v}\right)^3 + 0.115\left(\frac{b}{v}\right)^4. \tag{17}$$

The rate of vapor evaporation and condensation per unit area per unit time ($\dot{m}$) of the cavitation bubble is expressed as[32]

$$\dot{m} = \frac{\alpha_M}{(2\pi R_V)^{1/2}}\left(\frac{P_V^*}{T_0^{1/2}} - \frac{KP_V}{T^{1/2}}\right), \tag{18}$$

where α_M is the accommodation coefficient for evaporation or condensation (assumed constant), R_V the gas constant of water vapor, P_V^* the saturated vapor pressure, and P_V the partial pressure of water vapor in the bubble

$$P_V = \frac{n_{\text{H}_2\text{O}}P_{\text{in}}(t)}{\left(n_{\text{H}_2\text{O}} + n_{\text{air}}\right)}. \tag{19}$$

The correction facto K is expressed as[15]

$$K = \mathrm{e}^{(-\Omega^2)} - \Omega\sqrt{\pi}\int_0^{\pi} \mathrm{e}^{(-x^2)}\,\mathrm{d}x, \tag{20}$$

in which

$$\Omega = \frac{\dot{m}}{P_{\mathrm{V}}}\left(\frac{R_{\mathrm{V}}T}{2}\right)^{1/2}. \tag{21}$$

The amount of water vapor ($n_{\mathrm{H_2O}}$) changes with time by evaporation or condensation[15] is given as follows:

$$n_{\mathrm{H_2O}}(t+\Delta t) = n_{\mathrm{H_2O}}(t) + \frac{N_{\mathrm{A}}}{M_{\mathrm{H_2O}}} 4\pi R^2 \dot{m}\Delta t. \tag{22}$$

3. Results and discussion

In this work, the dynamic characteristics of a single bubble in a spherical bubbles' cluster in a finite volume of an unbounded compressible viscous liquid, are investigated. In our analysis, the complex interplay of bubble interactions, as well as the evaporation and condensation of water vapor is considered. To solve the dynamic equation, the widely used Runge–Kutta method is used and the following physical parameters are set: $T_0 = 293$ K, $P_{\mathrm{v}}^* = 2338$ Pa, $c = 1483$ m/s, $\sigma = 7.275\times10^{-2}$ N/m, $\mu = 1\times10^{-3}$ Pa·s, $\rho = 998.2$ kg/m^3, and $P_0 = 101325$ Pa. We mainly investigate the time-varying characteristics of various parameters such as normalized radius, internal pressure, internal energy, internal temperature, and the number of water vapor molecules inside an individual bubble, located at the different positions of the bubble cluster excited by ultrasound.

3.1. Effect of bubble state on bubble dynamic

3.1.1. Single bubble and bubbles in a cluster

To study the dynamic characteristics of a bubble in the cluster of bubbles, we investigate the bubble motion in the center and at the surface of the cluster by using Eq. (1). The calculation results are shown in Fig. 1.

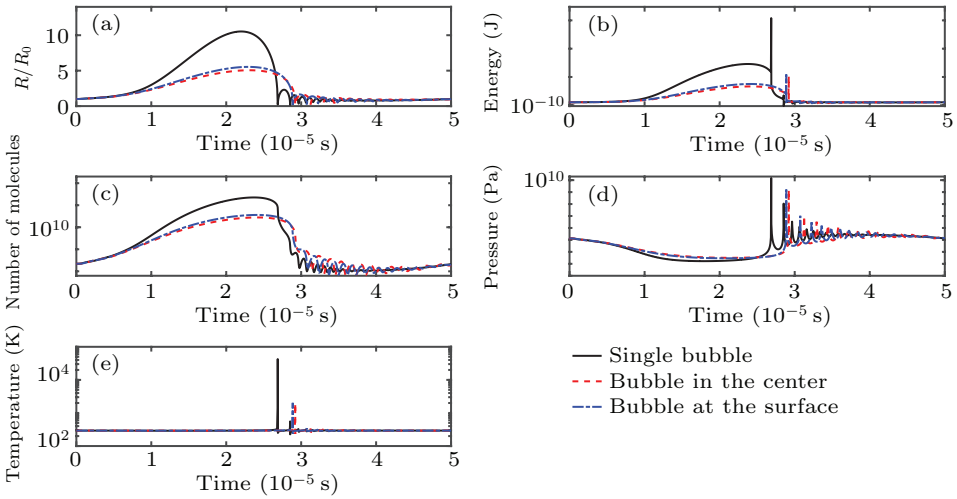


Fig. 1. Dynamical behaviors of a single bubble, a bubble in the center of bubble cluster, and a bubble at surface of bubble cluster, showing time-dependent (a) normalized radius for bubble, (b) energy in bubble, (c) number of water molecules in bubble, (d) pressure in bubble, (e) temperature in bubble, with frequency of ultrasound being 20 kHz, amplitude of ultrasound pressure 1.2 atm (1 atm = 1.01325×10^5 Pa), ambient bubble radius 4.5 μm, radius of cluster 1 mm, and total number of bubbles in cluster 300.

Figure 1(a) displays a bubble oscillating with its expansion and contraction, indicating the typical dynamics of a single bubble in an unbounded liquid versus a bubble in a monodisperse cluster. The results show that the expansion ratio of a single bubble is significantly greater than that of a bubble in a cluster, and the expansion ratio of a bubble in the center of the cluster is slightly smaller than that of a bubble at the surface. As each bubble absorbs acoustical energy from external source, it repeatedly releases secondary radiation pressure waves that act on surrounding bubbles,[27] suppressing the radial pulsations of each bubble. Compared with a bubble in a cluster, a single bubble has a shorter expansion time and undergoes a more violent collapse due to the lack of inhibition of secondary force, which contributes to accelerating the collapse when the bubble bursts. The internal energy and the number of water molecules in the bubble varying with time are shown in Figs. 1(b) and 1(c), respectively. It should be noted that in Figs. 1(b) and 1(c), the vertical axis is logarithmically scaled. During the slow expansion phase, the internal pressure of bubble decreases, leading to a rapid increase in the number of molecules present. However, when the bubble collapses, the internal pressure drastically increases, resulting in a sharp decline in the number of molecules. After this initial decline, the bubble radius undergoes small oscillations, leading to minor fluctuations in the number of vapor molecules present.[15] During bubble collapse, the energy in the bubble rises sharply due to the large amount of work done by the surrounding liquid. Figures 1(b) and 1(c) show that the internal energy of a single bubble is significantly greater than that of a bubble located at the surface or in the center of a cluster. Additionally, the maximum number of water molecules inside a single bubble is considerably more than that inside a bubble in a cluster.

During the expansion phase, the bubble in a cluster has lower internal pressure, and its ability to absorb vapor molecules is weaker than that of the single bubble. Figure 1(d) shows the variation in internal pressure of a bubble with time in a logarithmic coordinate. It can be seen that the pressure inside the bubble precipitously decreases at the beginning of the expansion due to a sudden increase in the volume of the bubble, and then slowly declines with a multitude of water molecules entering into the bubble and contributing the partial pressure of vapor molecules until the bubble collapses. Figure 1(e) exhibits the variation in internal temperature of a bubble with time. During the expansion phase, the internal temperature of the bubble is almost constant, which indicates that the expansion of the bubble is an isothermal process, whether a single bubble or a bubble is in a bubble cluster. When the bubble collapses, the maximum internal temperature of the single bubble is much higher than that of the bubble in a cluster. This is because the single bubble absorbs more energy-carrying water molecules during the expansion phase, and the absorption of this energy is too late to dissipate when the bubble collapses, thus forming a higher local temperature.

3.1.2. Radius of cluster

Figure 2 illustrates the influence of the radius of cluster on the characteristic of bubble at the cluster center with time. Figure 2(a) shows the normalized radius of bubble in the cluster center varying with time. It is evident that the expansion ratio of the bubble in a larger cluster is larger. Additionally, the expansion time and the collapse time of the bubble in a smaller cluster are both longer. The large radius of the bubble cluster indicates that the density of bubbles in the cluster is small, which further means that the bubbles are less restricted by other bubbles. Figure 2(b) illustrates the internal energy in the bubble varying with time. It can be seen that the energy inside the bubble in cluster with relatively large radius changes violently with time and reaches a larger peak when collapsing. Figure 2(c) shows the number of molecules in the bubble changing with time. It can be seen that the change trend of the number of water molecules in the bubble with time is almost consistent with that of the bubble radius with time. Figures 2(d) and 2(e) demonstrate the time-dependent internal pressures and temperatures of the bubbles in the center of the clusters with different radii, respectively. It can be seen that the radius of the cluster has little effect on the internal energy and temperature of the bubble. The larger the radius of the cluster, the larger the maximum radius that the bubble can reach, so that at the expansion phase, more water vapor molecules enter into the inside of the bubble, making the internal energy of the bubble increase, but at bubble collapse, there will be more vapor molecules too late to condense, so the temperature in the bubble will not be affected.

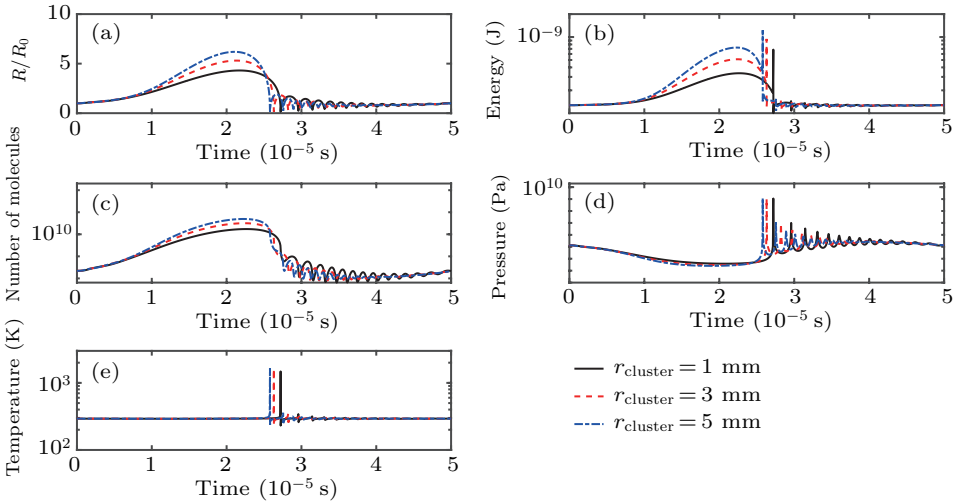


Fig. 2. Dynamic characteristics of bubbles in centers of clusters with different radii, showing time-dependent (a) normalized radius, (b) energy in bubble, (c) number of water molecules in bubble, (d) pressure in bubble, (e) temperature in bubble, with frequency of ultrasound being 20 kHz, amplitude of the ultrasound pressure 1.2 atm, ambient bubble radius 4.5 μm, initial number of water molecules and gas molecules in the bubble 2.20415×10^8 and 1.23822×10^{10}, respectively, radii of the cluster 1 mm, 3 mm, and 5 mm, respectively, and the total number of bubbles in cluster 300.

3.1.3. Number and relative position of bubbles

Figure 3 illustrates the dynamic characteristics of bubbles at various positions within the bubble cluster, exhibiting the variations in the maximum expansion ratio of bubbles in a cluster consisting of N bubbles ($N = 300$, 500, 1000), with the distance of the bubble from the center of the cluster. We chose 300, 500, and 1000 as the number of bubbles in the cluster because the ratio of the sum of the volumes of these bubbles at their maximum expansion to the volume of the bubble cluster is within a reasonable range. The maximum expansion ratio $R_{\max}/R_0$ of the bubble is directly proportional to the distance r_0 of the bubble from the center of the cluster. Furthermore, the slope of the curve increases as the distance r_0 increases, indicating that the growth rate of the maximum expansion radius also increases. When the radius of the bubble cluster is kept constant, the value of $R_{\max}/R_0$ decreases as the number

of bubbles in the cluster increases. This implies that an increase in the density of bubbles in the cluster suppresses the expansion of the bubbles.

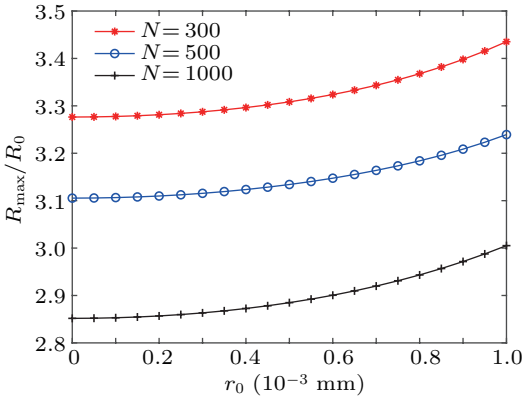


Fig. 3. Dynamic characteristics of bubbles at different positions in bubble cluster, with frequency of ultrasound being 20 kHz, amplitude of ultrasound pressure 1.2 atm, ambient bubble radius 4.5 μm, initial number of water molecules and gas molecules in bubble 2.20415×10^8 and 1.23822×10^{10}, respectively, the radius of cluster 1 mm, and the total number of bubbles in cluster 300, 500, and 1000, respectively.

3.2. Effect of acoustic field parameters on bubble dynamic

3.2.1. Driving acoustic frequency

Figure 4 shows the dynamic characteristics of a bubble located in the center of the cluster at different ultrasonic frequencies.

Figure 4(a) illustrates the variations in the normalized radius of the bubble with time. It is observable that the expansion ratio and oscillation frequency of the bubble decrease as the driving frequency increases. At a driving frequency of $f = 20$ kHz, the bubble oscillates thrice in a cycle, whereas at $f = 30$ kHz and $f = 50$ kHz, the bubble oscillates thrice and only once in a cycle, respectively. This is due to the fact that smaller bubbles have a stronger acoustic response to low-frequency ultrasound. Figures 4(b)–4(e) respectively show the variations of the internal energy, temperature, pressure, and the number of water molecules in the bubble with time. It can be observed that the internal energy, internal pressure, and internal temperature in the bubble reach their peak points at the moment of bubble bursting. As the bubble expands to its maximum size, the number of water molecules within the bubble also reaches its maximum. The maximum values of internal energy, temperature, pressure, and the number of water molecules in the bubble decrease as the ultrasonic frequency increases. This phenomenon can be easily explained by the fact that the negative phase duration is relatively short when the ultrasonic frequency is high. Consequently, there is less time for the bubble to expand and accumulate water vapor molecules, resulting in less internal energy and lower internal temperature and pressure.

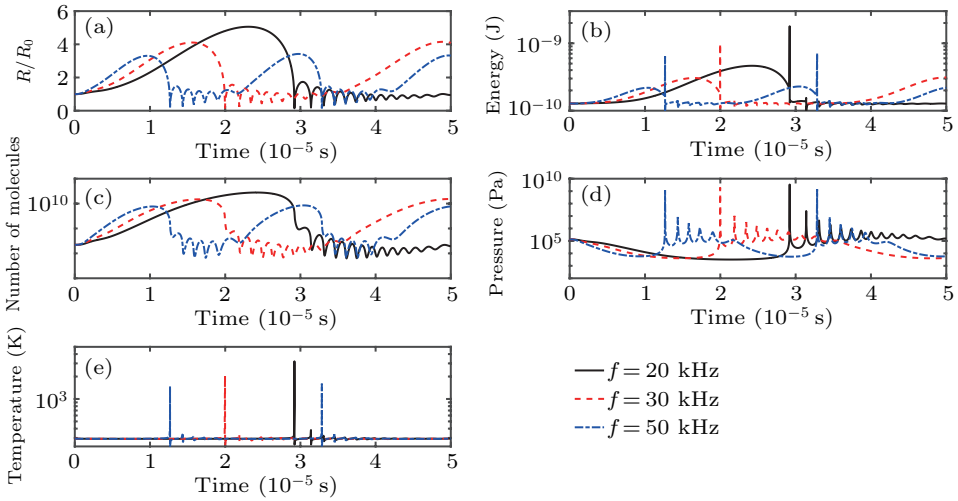


Fig. 4. Dynamic characteristics of bubbles with different ambient radii in bubble cluster, showing time-dependent (a) normalized radius, (b) energy in the bubble, (c) number of water molecules in the bubble, (d) pressure in the bubble, (e) temperature in the bubble, with frequencies of ultrasound being 20 kHz, 30 kHz, and 50 kHz, respectively, amplitude of ultrasound pressure 1.2 atm, ambient bubble radius 4.5 μm, initial number of water molecules and gas molecules in the bubble 2.20415×10^8 and 1.23822×10^{10}, respectively, radius of cluster 1 mm, and total number of bubbles in cluster 300.

3.2.2. Driving acoustic pressure

Figure 5 shows the dynamic characteristics of the bubble in the center of the cluster at different acoustic pressures.

Figure 5(a) shows the time-dependent normalized radius of the bubble, illustrating the oscillation amplitude, maximum bubble radius, and collapse time increasing with ultrasonic pressure rising. Figures 5(b)–5(e) show the variations of internal energy, internal pressure, internal temperature, and the number of water molecules in the bubble with time going by. Notably, we observe that the maximum internal energy, pressure, temperature, and number of water molecules are all increase with driving pressure rising. At relatively high acoustic amplitudes, the bubble absorbs more energy during the rarefaction phase of ultrasound, causing the bubble wall to experience a larger pressure difference, resulting in greater amplitude expansion. Consequently, during the expansion phase,

the internal pressure is lower, and the rate of evaporation of water vapor molecules is faster, ultimately resulting in more water vapor molecules possessing the bubble and higher internal energy, pressure, and temperature at bubble collapse.

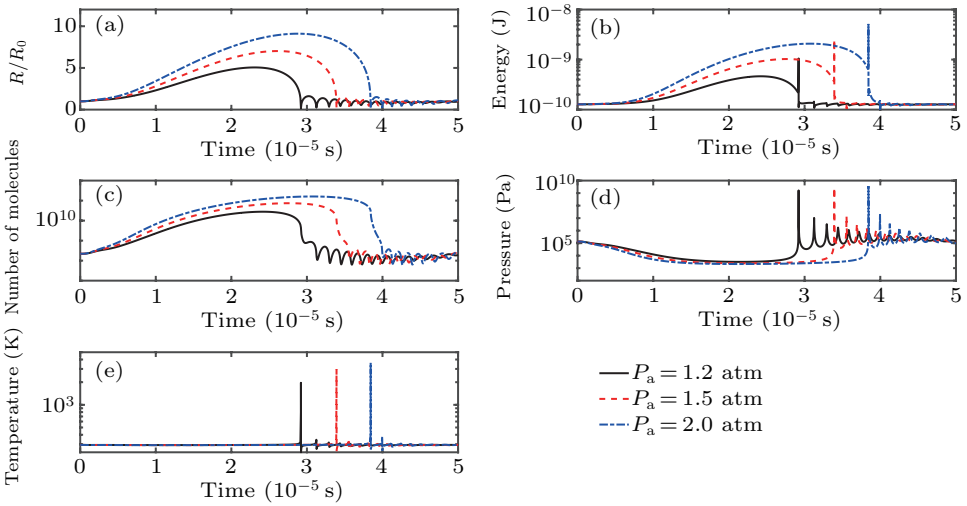


Fig. 5. Dynamic characteristics of the bubbles with different ambient radii in bubble cluster, showing time-dependent (a) normalized radius, (b) energy in bubble, (c) number of water molecules in bubble, (d) pressure in bubble, (e) temperature in the bubble, with frequency of ultrasound being 20 kHz, amplitudes of ultrasound pressures 1.2 atm, 1.5 atm, and 2.0 atm, respectively, ambient bubble radius 4.5 μm, initial number of water molecules and gas molecules in bubble 2.20415×10^8 and 1.23822×10^{10}, respectively, radius of cluster 1 mm, and total number of bubbles in the cluster 300.

3.2.3. Driving acoustic waveform

To investigate the dynamic characteristics of bubbles driven by ultrasonic waves with different waveforms, we employ three types of driving acoustic waves: sinusoidal wave, rectangular wave, and triangular wave, as shown in Fig. 6. The approximate expression of the rectangular wave and the triangular wave are given as follows:[33]

$$P_r = P_a \sum_{j=0}^{4} \frac{4}{(2j+1)\pi} \sin[2\pi(2j+1)ft], \tag{23}$$

$$P_t = P_a \sum_{j=0}^{4} \frac{8(-1)^j}{(2j+1)^2\pi^2} \sin[2\pi(2j+1)ft]. \tag{24}$$

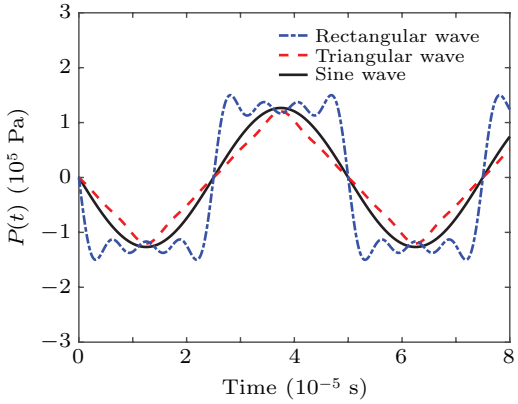


Fig. 6. Waveforms of three types of driving ultrasound waves.

The calculation results of three types of ultrasounds driving the bubble under same pressure are shown in Fig. 7. Figure 7(a) shows the curves of the normalized bubble radius changing with time, indicating that different waveforms have distinct effects on bubble expansion. Specifically, the bubble driven by the rectangular wave expands more than the bubble driven by the sinusoidal wave, whereas the bubble driven by the triangular wave exhibits the opposite trend. Furthermore, figure 7(a) illustrates that the expansion velocity at the initial stage varies with waveform. The bubble driven by the rectangular wave first expands rapidly and slows down around $t = 7$ μs, while the bubble driven by the triangular or sinusoidal wave shows a slow-to-fast trend. The reason can be attributed to the difference in pressure profile among different waveforms as shown in Fig. 6. The rectangular wave has a peak pressure value that is reached quickly, which is followed by a series of small oscillations, whereas the pressure of the triangular wave or sinusoidal wave grows slowly. Figures 7(b)–7(e) display the change curves of time-dependent internal energy, internal pressure, internal temperature, and the number of water molecules inside the bubble. The simulation results indicate that the bubble exchanges more mass and energy, with the rectangular wave driven, but not and the exchange is restricted, with the triangular wave driven. The cavitation effect, according to Ref. [9], can be effectively enhanced by reducing the frequency difference between the two ultrasonic waves and the proportion of high-frequency acoustic power. On the other hand, the phase difference in a range from $\pi/2$ to $5\pi/4$ may result in a lower acoustic cavitation effect. In Eqs. (23) and (24), it can be seen that rectangular wave and the triangular wave adopted in this work can be regarded as the modulation of sinusoidal waves of different frequencies.

The power proportion of rectangular wave is mainly concentrated in the low-frequency component and it can effectively enhance the cavitation effect. The difference in phase between sinusoidal waves that constitute the triangular wave is π and the triangular wave can suppress the cavitation effect. These results are consistent with the conclusions in Ref. [35].

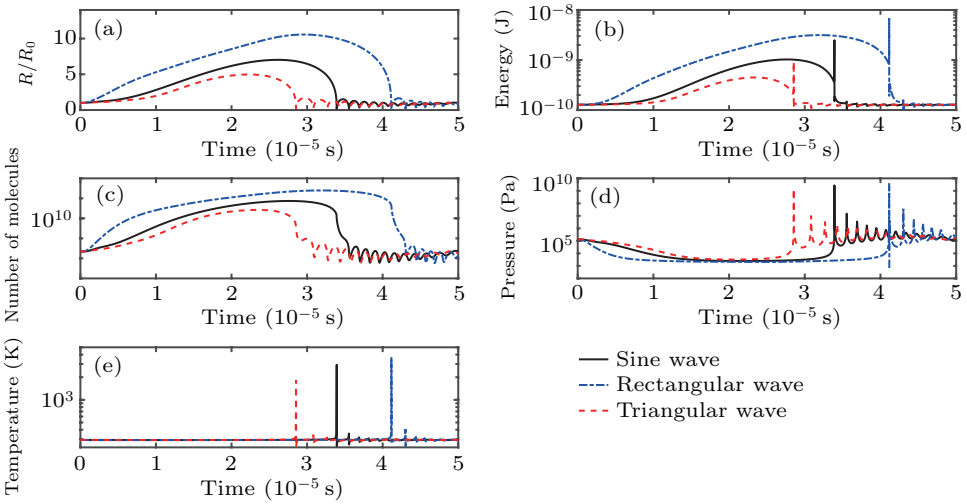


Fig. 7. Dynamic characteristics of bubbles with different ambient radii in the bubble cluster, showing time-dependent (a) normalized radius, (b) energy in bubble, (c) number of water molecules in bubble, (d) pressure in bubble, (e) temperature in bubble, with frequency of ultrasound being 20 kHz, amplitude of ultrasound pressure 1.2 atm, ambient bubble radius 4.5 μm, initial number of water molecules and gas molecules in bubble 2.20415×10^{8} and 1.23822×10^{10}, respectively, radius of the cluster 1 mm, and total number of bubbles in cluster 300.

3.3. Effect of evaporation and condensation of vapor

Figure 8 shows the calculation results of the bubble cluster dynamic characteristics with or without evaporation and condensation of vapor. Figure 8(a) shows that the maximum expansion ratio of the bubble increases slightly in the model with evaporation and condensation of vapor. Figure 8(b) displays that the energy inside the bubble is significantly different in the expansion stage of the bubble. During the expansion phase, the pressure inside the bubble decreases (see in Fig. 8(c)), and after taking into account the mass exchange, water molecules carrying energy will enter the bubble, resulting in energy increasing inside the bubble. Figures 8(c) and 8(d) show the internal pressure and internal temperature of bubble varying with time, respectively. It can be seen that considering the evaporation and condensation of steam, the maximum pressure and maximum temperature of the bubble will decrease, especially the temperature decrease will be more obvious. This is because the temperature is very high at the moment of bubble collapse, and the pressure increases instantaneously, resulting in the rapid condensation of a large amount of water vapor, and the energy taken away by each water vapor molecule is large, so that the temperature inside the bubble is greatly reduced. However, comparing with single bubble,[34] the effect of evaporation and condensation of vapor on the dynamic characteristics of multi-bubble are not so significant, because the bubble–bubble interactions inhibit the energy-carrying water molecules from entering into the bubble.

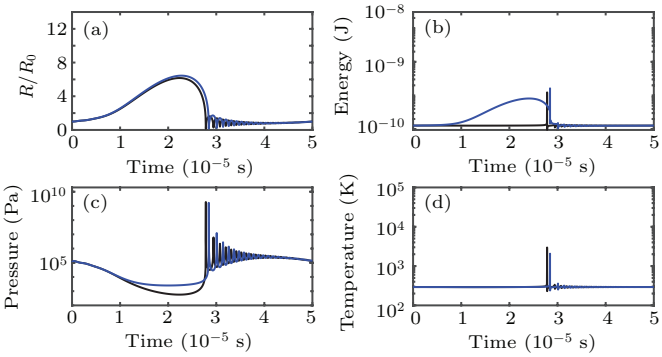


Fig. 8. Dynamic characteristics of bubbles with different ambient radii in bubble cluster, showing time-dependent (a) normalized radius, (b) energy in bubble, (c) pressure in bubble, (d) temperature in bubble, with solid black lines representing the calculation results of the model without evaporation condensation of vapor, dash-dotted lines denoting calculation results of model with evaporation and condensation of vapor, with frequency of ultrasound being 20 kHz, amplitude of ultrasound pressure 1.2 atm, ambient bubble radius 4.5 μm, initial number of water molecules and gas molecules in bubble 2.20415×10^{8} and 1.23822×10^{10}, respectively, the radius of cluster 1 mm, and total number of bubbles in cluster 100.

4. Conclusions

In this work, a dynamic model of bubbles in a spherical bubble cluster is established by considering the evaporation and condensation of water vapor and the interaction between bubbles. The influences of the position and ambient radius of bubbles and the number of bubbles in the bubble cluster on the dynamic characteristics of the cavitation bubble are discussed. Additionally, the changes of the normalized radius of the bubble, energy, temperature, pressure, and the number of water vapor molecules in the bubble cluster are studied under different ultrasound waves. Our findings lead to the following

conclusions.

(i) The dynamic characteristics of bubble in a cluster are affected by the surrounding bubbles and they are also affected by the position of bubble in the cluster.

(ii) The radius of the cluster considerably affects the dynamic characteristics of bubble. The large cluster promotes the mass exchange inside and outside the bubble, but has little effect on the energy exchange.

(iii) Increasing the number of bubbles in the cluster can enhance the interaction between bubbles, further leading to the cavitation activities to be suppressed.

(iv) The frequency, pressure, and waveform of the driving wave can also significantly affect cavitation activities. As the ultrasonic frequency decreases and the pressure increases in a certain range, the bubble oscillates more violently. Under the same ultrasonic frequency and pressure, the rectangular wave enhances the cavitation of the bubbles in the clusters, while the triangular wave weakens the cavitation of the bubbles in the clusters. The rectangular wave prolongs the expansion time of bubble, while the triangular wave reduces the expansion time. The waveform of the driving ultrasound has a great influence on the mass exchange and energy exchange inside and outside the bubble.

(v) The mass transfer inside and outside the bubble affects the state of the bubble when it collapses, especially the maximum temperature reduction is more obvious.

Our investigation fills the gap of bubble cluster dynamics model considering evaporation and condensation of vapor, and has certain theoretical guiding significance for ultrasonic cavitation experiment, environmental engineering application, and the design of sonochemistry reactor. It should be noted that in the process of establishing the bubble dynamics model in this work, we assume that all bubbles have the same initial radius and that they are evenly distributed in the cluster. However, in practical applications, the sizes of cavitation bubbles are polydisperse, and different initial radii of bubbles have different effects on surrounding bubbles.[29] In addition, the translation and non-spherical oscillation of the bubbles are also ignored.[36] In the future, we will continue to optimize the model and investigate the effects of translation, non-sphericity, and size polydispersity of the bubble.

Acknowledgement

Project supported by the National Natural Science Foundation of China (Grant No. 12074354).

References

[1] Zhang X M, Li F, Wang C H, Hu J, Mo R Y, Shen Z Z, Guo J Z and Lin S Y 2023 *Chin. Phys. B* **32** 064303
[2] Li M, Manica R, Xiang B and Liu Q 2021 *Chem. Eng. Sci.* **246** 116997
[3] Ma X, Huang B, Zhao X, Wang Y, Chang Q, Qiu S, Fu X and Wang G 2018 *Ultrason. Sonochem.* **43** 80
[4] Liang J F, Xiong D F, An Y and Chen W Z 2022 *Chin. Phys. B* **31** 117802
[5] Pflieger R, Nikitenko S I and Ashokkumar M 2019 *Ultrason. Sonochem.* **59** 104753
[6] Theerthagiri J, Madhavan J, Lee S J, Choi M Y, Ashokkumar M and Pollet B G 2020 *Ultrason. Sonochem.* **63** 104960
[7] Hu J W, Wang L M, Qian S Y, Liu W Y, Liu Y T and Lei W R 2019 *Chin. Phys. B* **28** 114301
[8] Bhangu S K, Bocchinfuso G, Ashokkumar M and Cavalieri F 2020 *Nanoscale Horiz.* **5** 553
[9] Shanei A,Akbari-Zadeh H, Attaran N, Salamat M R and Baradaran-Ghahfarokhi M 2020 *Ultrasonics* **102** 106061
[10] Plesset M S 1949 *J. Appl. Mech.* **16** 277
[11] Shen Y, Yasui K, Zhu T and Ashokkumar M 2017 *Phys. Chem. Chem. Phys.* **19** 20635
[12] Shen Y, Pflieger R, Chen W Z and Ashokkumar M 2023 *Utrason. Somochem.* **93** 106307
[13] Poritsky H and Horvay G 1952 *J. Appl. Mech.* **19** 229
[14] Keller J B and Miksis M J 1980 *J. Acoust. Soc. Am.* **68** 628
[15] Yasui K 1995 *J. Acoust. Soc. Am.* **98** 2772
[16] Lu Y, Ge Z, Li X, Shen D, Kang Y and Chen J 2009 *J. Chin. U. Min. Technol.* **38** 582
[17] Gao X, Chen W, W. Huang, Xu J, Xu X, Liu Y and Liang Y 2009 *Chinese Sci. Bull.* **54** 408
[18] Cogne C, Labouret S, Peczalski R, Louisnard O, Baillon F and Espitalier F 2016 *Ultrason. Sonochem.* **29** 447
[19] Liao J, Tan J, Peng L and Xue H 2023 *Ultrason. Sonochem.* **100** 106614
[20] Suo D, Govind B, Zhang S and Jing Y 2018 *Ultrason. Sonochem.* **41** 419
[21] Wang Y, Chen D and Wu P 2023 *Ultrason. Sonochem.* **99** 106585
[22] Mettin R, Akhatov I, Parlitz U, Ohl C and Lauterborn W 1977 *Phys. Rev. E* **56** 2924
[23] Doinikov A A 2021 *Phys. Rev. E* **64** 026301
[24] Zou Q, Lei S, Zhang Y and Dui Q 2023 *Chin. Phys. B* **32** 014302
[25] Pelekasis N A, Gaki A, Doinikov A and Tsamopoulos J A 2004 *J. Fluid Mech.* **500** 313
[26] Jiao J, He Y, Kentish S E, Ashokkumar M, Manasseh R and Lee J 2015 *Ultrasonics* **58** 35
[27] Shen Y, Zhang L, Wu Y and Chen W 2021 *Ultrason. Sonochem.* **73** 105535
[28] Qin D, Yang Q, Lei S, Fu J, Ji X and Wang X 2023 *Ultrason. Sonochem.* **99** 106586
[29] Zou Q, Zhong X, Zhang B, Gao A, Wang X, Li Z and Qin D 2023 *Ultrasonics* **134** 107809
[30] An Y 2011 *Phys. Rev. E* **83** 066313
[31] Yasui K 1996 *J. Phys. Soc. Jpn.* **65** 2830
[32] Yasui K 1997 *Phys. Rev. E* **56** 6750
[33] Chen W, Chen X, Lu M, Miao G and Wei R 2002 *J. Acoust. Soc. Am.* **111** 2632
[34] Shen Y, Zhu T, You M, MEI B, Han J, Xie Y, Li X and Yasui K 2015 *J. Chem. Eng. Chin. U.* **04** 809185
[35] Kaouther K and Oualid H 2018 *Ultrason. Sonochem.* **42** 508
[36] Wu X and Liang J 2021 *Acta Phys. Sin.* **70** 184301 (in Chinese)